

## Microscopic Cords, a Virulence-Related Characteristic of *Mycobacterium tuberculosis*, Are Also Present in Nonpathogenic Mycobacteria<sup>∇†</sup>

Esther Julián,<sup>1</sup> Mónica Roldán,<sup>2</sup> Alejandro Sánchez-Chardi,<sup>2</sup> Oihane Astola,<sup>1</sup>  
Gemma Agustí,<sup>1</sup> and Marina Luquin<sup>1\*</sup>

Departament de Genètica i de Microbiologia, Facultat de Biociències, Universitat Autònoma de Barcelona, 08193 Bellaterra (Barcelona), Spain,<sup>1</sup> and Servei de Microscòpia Electrònica, Universitat Autònoma de Barcelona, 08193 Bellaterra (Barcelona), Spain<sup>2</sup>

Received 12 November 2009/Accepted 14 January 2010

**The aggregation of mycobacterial cells in a definite order, forming microscopic structures that resemble cords, is known as cord formation, or cording, and is considered a virulence factor in the *Mycobacterium tuberculosis* complex and the species *Mycobacterium marinum*. In the 1950s, cording was related to a trehalose dimycolate lipid that, consequently, was named the cord factor. However, modern techniques of microbial genetics have revealed that cording can be affected by mutations in genes not directly involved in trehalose dimycolate biosynthesis. Therefore, questions such as “How does mycobacterial cord formation occur?” and “Which molecular factors play a role in cord formation?” remain unanswered. At present, one of the problems in cording studies is the correct interpretation of cording morphology. Using optical microscopy, it is sometimes difficult to distinguish between cording and clumping, which is a general property of mycobacteria due to their hydrophobic surfaces. In this work, we provide a new way to visualize cords in great detail using scanning electron microscopy, and we show the first scanning electron microscopy images of the ultrastructure of mycobacterial cords, making this technique the ideal tool for cording studies. This technique has enabled us to affirm that nonpathogenic mycobacteria also form microscopic cords. Finally, we demonstrate that a strong correlation exists between microscopic cords, rough colonial morphology, and increased persistence of mycobacteria inside macrophages.**

*Mycobacterium tuberculosis*, the causative agent of human tuberculosis (TB), killed 1.5 million people in 2006. A further 200,000 HIV-positive people died from HIV-associated TB (<http://www.who.int/tb/en/index.html>). Intensive research into the virulence factors that determine the pathogenicity of *M. tuberculosis* have been carried out since the tubercle bacillus was discovered. Unfortunately, despite the knowledge obtained, the factors that make *M. tuberculosis* virulent have not yet been identified (23, 29). One of the first phenotypic characteristics linked to virulence was the microscopic formation of cords. When *M. tuberculosis* cells grow in a liquid medium without detergent, they form tight bundles, or cords, consisting of bacilli in which the orientation of the long axis of each cell is parallel to the long axis of the cord. *M. tuberculosis* microscopic cords were first observed by Robert Koch in 1882, but knowledge of their significance increased in 1947 with studies by Middlebrook et al. (16). These authors compared the virulent H37Rv and avirulent H37Ra *M. tuberculosis* strains and found that the formation of cords took place only in the virulent strain, whereas cells from the avirulent H37Ra strain were not oriented and merely formed irregular clumps. In 1953, Bloch isolated a toxic glycolipid from *M. tuberculosis* and re-

lated it to the virulence of the tubercle bacillus and to cording. Bloch named the glycolipid cord factor, and later, it was identified as trehalose dimycolate (TDM) (2, 17). However, 56 years after Bloch's description, we know that TDM is not the cording factor, as multiple alterations in cell envelopes unrelated to TDM can lead to loss of cording (see reference 8 for an excellent review). Furthermore, all the *Mycobacterium* spp. researched to date (pathogenic and nonpathogenic, with the exception of *M. leprae*, which has only trehalose monomycolate [5]) have TDM in their cell walls (8).

The formation of microscopic cords has also been described in *M. marinum*, a fish, amphibian, and opportunistic human pathogen that is phylogenetically related to members of the *M. tuberculosis* complex (11, 24, 25). Genetic validation of the link between cording and virulence was obtained by means of the construction of transposon mutants in strains of both the *M. tuberculosis* complex and the species *M. marinum* (8).

A recent occurrence with *M. abscessus* has strengthened the argument for the relationship between cording and virulence. Smooth *M. abscessus* colonies can switch to rough colonies, and interestingly, the rough morphotype formed microscopic cords in a liquid medium and was more virulent than the smooth morphotype in human monocytes and in a mouse TB model (12). Smooth colonies did not form cords in liquid medium and contained large amounts of cell wall glycopeptidolipids that were present in only minimal amounts in rough cording types (12). The authors concluded that the ability to switch from smooth noncording to rough cording morphotypes may allow *M. abscessus* to make the transition between a colonizing phenotype and a more virulent invasive form. This is a

\* Corresponding author. Mailing address: Departament de Genètica i de Microbiologia, Facultat de Biociències, Universitat Autònoma de Barcelona, 08193 Bellaterra (Barcelona), Spain. Phone: (34) 93 581 2540. Fax: (34) 93 581 2387. E-mail: marina.luquin@uab.cat.

† Supplemental material for this article may be found at <http://jb.asm.org/>.

∇ Published ahead of print on 22 January 2010.

very interesting hypothesis, supported by the findings of Cathérinot et al. (3), who reported a case of acute respiratory failure involving a rough variant of *M. abscessus*. Another correlation can be made from these findings, between rough colonies and cording, since only rough colonies of *M. abscessus* formed microscopic cords, and cording *M. tuberculosis* and *M. marinum* strains displayed only rough colonies.

In previous works, we obtained spontaneous rough-colony mutants from the species *M. chubuense*, *M. gilvum*, *M. obuense*, *M. parafortuitum*, and *M. vaccae*. As we have previously reported, in all these species, colonies with both smooth and rough morphologies produced TDM in similar amounts, and no differences were found in the patterns of the other cell wall glycolipids and mycolic acids (1). However, smooth colonies synthesized a saturated polyester that was absent in rough colonies (1, 21). This compound is a long-chain saturated fatty acid polyester of estolide-like structure containing mainly C<sub>16:0</sub> and C<sub>18:0</sub> saturated acids linked to C<sub>14</sub>, C<sub>16</sub>, and C<sub>18</sub> saturated alcohols (21).

*M. vaccae* was considered nonpathogenic until 1996, when it was described as the causal agent of pneumonia and cutaneous diseases (10). The other species studied are phylogenetically related to *M. vaccae* but are not considered to be pathogenic. All these species belong to the rapidly growing scotochromogenic mycobacteria (RGSM) group and are phylogenetically distant from *M. abscessus*, *M. marinum*, and the species of the *M. tuberculosis* complex (28). The relationship between microscopic cording and rough colonies in pathogenic species led us to study the formation of microscopic cords in the rough variants of these RGSM.

To date, cords have been detected only by optical microscopy. Using this technique, it is sometimes difficult to distinguish between cording and clumping, which is a general property of mycobacteria due to their hydrophobic surfaces. In this work, the formation of microscopic cords has been studied with scanning electron microscopy (SEM) for the first time in order to achieve the following main objectives: (i) to be able to affirm without the slightest doubt if a mycobacterial strain forms microscopic cords and (ii) to observe clearly the ultrastructure of cords and the organization of mycobacterial bacilli in these cords. We also used confocal laser scanning microscopy (CLSM) to obtain images of the colony structure. A comparison was made between both the structure of the colonies and the ultrastructure of the microscopic cords in the aforementioned strains of RGSM and the *M. marinum* type strain.

Microscopic cords today are considered to be related to virulence, so an interesting question is, if these rough colonial morphotypes produce microscopic cords, are they more virulent than the original smooth ones? In order to have a preliminary evaluation of this, we also researched the capacities of both rough and smooth mycobacteria to survive in murine macrophages.

#### MATERIALS AND METHODS

**Strains and growth medium.** The *M. chubuense* ATCC 27278<sup>T</sup>, *M. gilvum* DSM 43547, *M. obuense* ATCC 27023<sup>T</sup>, *M. parafortuitum* ATCC 19686<sup>T</sup>, and *M. vaccae* ATCC 15483<sup>T</sup> smooth strains and their respective rough natural mutants (obtained by us in previous works [1, 21]) were grown, together with the strain *M. marinum* ATCC 927<sup>T</sup>, on Trypticase soy agar (TSA) (Scharlau Chemie, Spain) medium for 2 weeks at 30°C. *M. marinum* was included as a positive control for

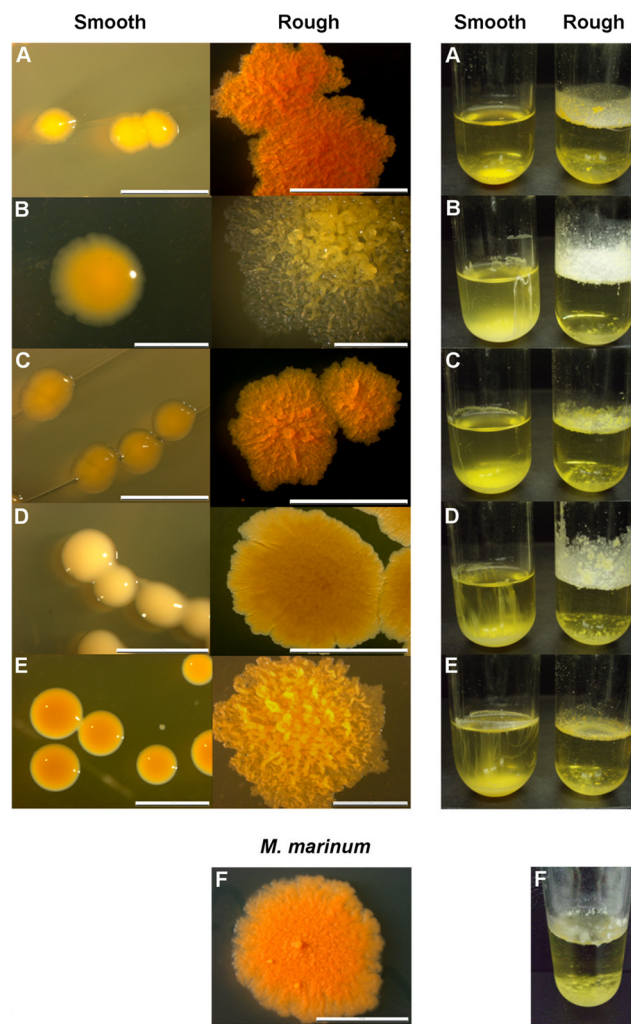


FIG. 1. Only rough colonies form spreading pellicles in TSB liquid medium. (A) *M. chubuense*. (B) *M. gilvum*. (C) *M. obuense*. (D) *M. parafortuitum*. (E) *M. vaccae*. (F) *M. marinum*. On the left are shown smooth and rough colonies grown on TSA plates. The colonies shown are representative of hundreds of colonies obtained throughout the study. On the right, the growth on TSB medium of an isolated colony taken from TSA is shown. For rough variants, the formation of spreading pellicles was observed in glass tubes. The size of the scale bars is 2 mm.

cording. The colonies obtained were studied by CLSM. For Ziehl-Neelsen smears and SEM studies of cords, one isolated colony was inoculated into Trypticase soy broth (TSB) (Scharlau Chemie, Spain), and the cultures were incubated (without shaking) at 30°C for 2 weeks.

**Optical microscopy.** In order to observe the morphology of the colonies grown on TSA, optical microscopy was performed using a Leica MZFLIII stereo microscope (Leica, Germany). Ziehl-Neelsen stains of spreading pellicles (for rough mutants) or sediments (for smooth mutants) that the mycobacteria formed in TSB were observed with a Leica-DMRBE microscope (Leica, Germany) equipped with differential interference contrast. Micrographs were taken using a DC 250 digital camera system.

**CLSM.** Colonies grown on TSA for 2 weeks were labeled with 10 µg/ml Hoechst 33342 (Molecular Probes) for 1 h at 37°C in the dark. The colonies were washed in 0.1 M phosphate-buffered saline (PBS) (Sigma-Aldrich, Germany) and mounted on Mat-Teck culture dishes (Mat Teck Corp., Ashland, MA).

Observations were made with a TCS-SP5 confocal laser scanning microscope (Leica, Germany) using a Plan Apo 40× (numerical aperture [NA], 1.25) oil objective. Hoechst 33342 DNA labels were excited with a blue diode (405 nm)



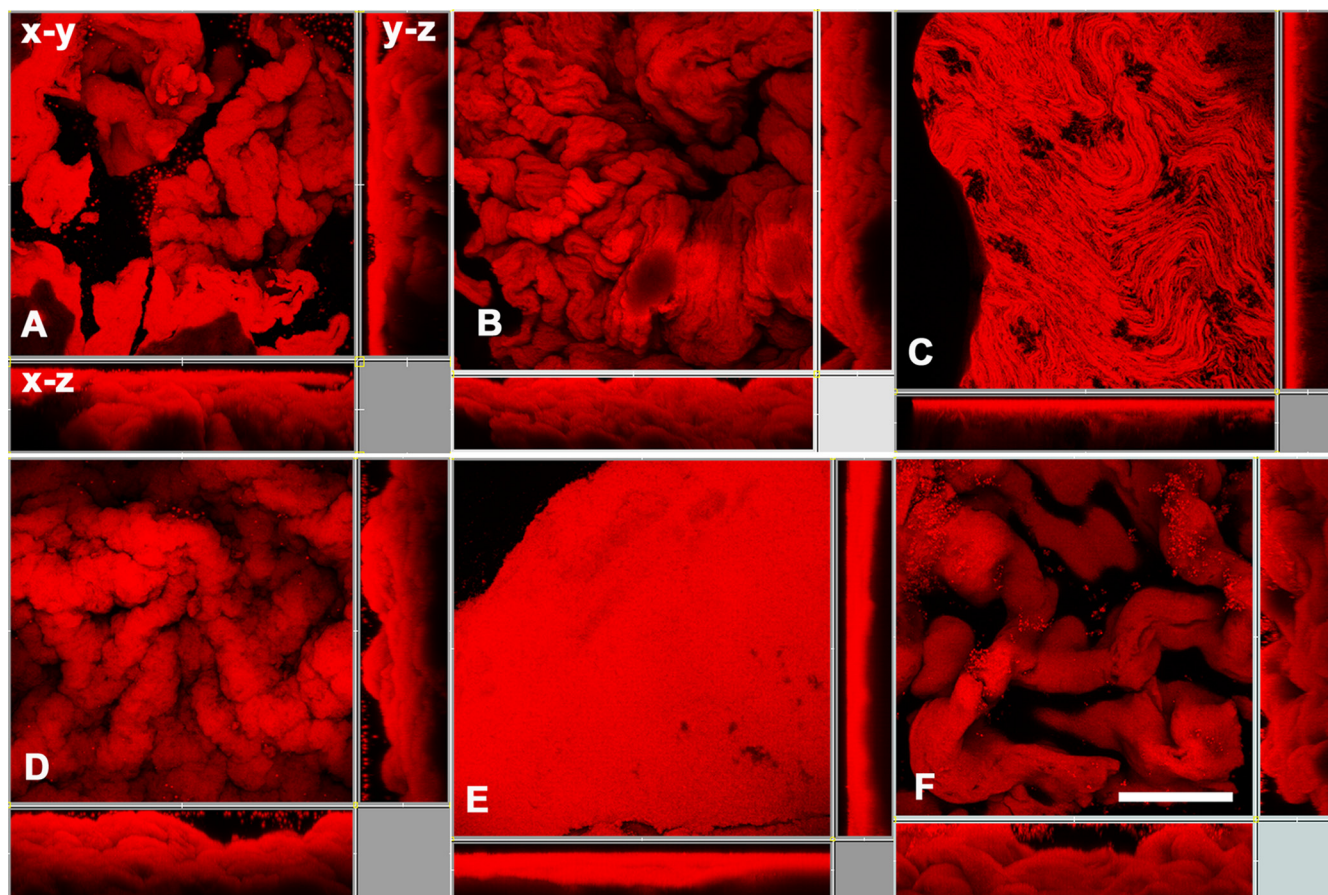


FIG. 2. Colonial cords are formed by the rough colonies of all of the species, with the sole exception of *M. parafortuitum*. Shown are CLSM micrographs of rough colonies grown on TSA with three-dimensional projections in *x-y*, *x-z*, and *y-z* views. (A) *M. chubuense*. (B) *M. gilvum*. (C) *M. marinum*. (D) *M. obuense*. (E) *M. parafortuitum*. (F) *M. vaccae*. The images are representative of the studies performed with colonies of four different cultures.

and detected in the 415- to 460-nm range. To determine the colony structure, a series of horizontal (*x-y*) optical sections were collected at 1- $\mu\text{m}$  intervals throughout the thickness of the colony. The projections of the series obtained were generated with Imaris v. 6.1.0. software (Bitplane, Switzerland) in order to visualize the structures formed by the bacteria in three dimensions. The 3 topographical images were obtained using LAS AF software (Leica, Germany).

**SEM of cells grown in TSB.** Cells for SEM studies were taken from spreading pellicles (for rough mutants) or sediments (for the smooth colonies) formed by mycobacteria in TSB. The pellicles or pellets were deposited on Nuclepore track-etch membranes with a pore size of 0.2  $\mu\text{m}$  (Whatman, United Kingdom). Duplicates of each sample were processed after air drying. One set of samples was fixed following conventional electron microscopy methods. In short, samples were fixed in 2.5% (vol/vol) glutaraldehyde in 0.1 M phosphate buffer (pH 7.4) for 2 h at 4°C, washed 4 times for 10 min each time in 0.1 M phosphate buffer, postfixed in 1% (wt/vol) osmium tetroxide with 0.7% ferrocyanide in phosphate buffer, washed in water, dehydrated in an ascending ethanol series (50, 70, 80, 90, and 95% for 10 min each and twice with 100% ethanol), and dried by critical-point drying with  $\text{CO}_2$ . This method enabled the samples to be well preserved, eliminating the main extracellular matrix and facilitating the observation of cells. The other set of samples was fixed directly with osmium vapor impregnation (12 h) and dried. This anhydrous method is a rapid and nondestructive technique that enables native and fragile structures with extracellular components to be conserved. All samples were mounted on adhesive carbon films and then coated with gold. Bacilli were observed with an S-570 scanning electron microscope (Hitachi Ltd., Japan) at an accelerating voltage of 15 kV.

**Infection of macrophages.** The murine macrophage J774 cell line was maintained in Dulbecco's modified Eagle's medium with L-glutamine (Gibco BRL), supplemented with 10% heat-inactivated fetal bovine serum (FBS) (Lonza Ltd.,

Switzerland), 100  $\mu\text{g/ml}$  streptomycin, and 100 U/ml penicillin at 37°C in an atmosphere containing 5%  $\text{CO}_2$ .

The bacterial colonies were scraped from TSA plates and suspended in PBS, slightly vortexed with glass beads, and allowed to settle for 30 min. The supernatant was adjusted to 1.0 McFarland standard. The cells were pelleted and resuspended in complete medium without antibiotics. Clumps of bacteria were disrupted by ultrasonic treatment of bacterial suspensions in an ultrasonic water bath as previously described (26). The disruption of bacterial clumps was further assessed microscopically. In a series of preliminary experiments, cell viability was tested after sonication for both smooth and rough variants of each mycobacterial species in order to verify the cell counts obtained in McFarland adjustments.

Macrophage cells ( $6 \times 10^5$  per well) were seeded onto 48-well tissue culture plates in complete medium without antibiotics, and 24 h later, they were infected with each of the different mycobacterial strains at a multiplicity of infection (MOI) of 100 for 3 h. After three successive washes with PBS to remove extracellular bacteria, the cells were incubated with fresh complete medium at 37°C. All infections were performed in triplicate. At different time points after infection (3, 8, 24, 48, 72, and 96 h), the cell culture supernatants were removed and the macrophages were lysed with 400  $\mu\text{l}$ /well of 0.1% Triton X-100 (Sigma-Aldrich, Germany). The bacterial counts in the cell lysates were determined in CFU by plating serial dilutions on TSA plates and incubating the cultures at 30°C for 2 weeks.

**Statistical analyses.** Data are presented as the mean  $\pm$  standard deviation (SD). First, data were log transformed and tested for both normal distribution (Kolmogorov-Smirnov) and homogeneity of variances (Levene). To determine if there were significant differences in the survival of smooth and rough variants inside J774 macrophages, an analysis of variance (ANOVA) was performed. Intergroup divergences at each time were calculated using the paired Student's

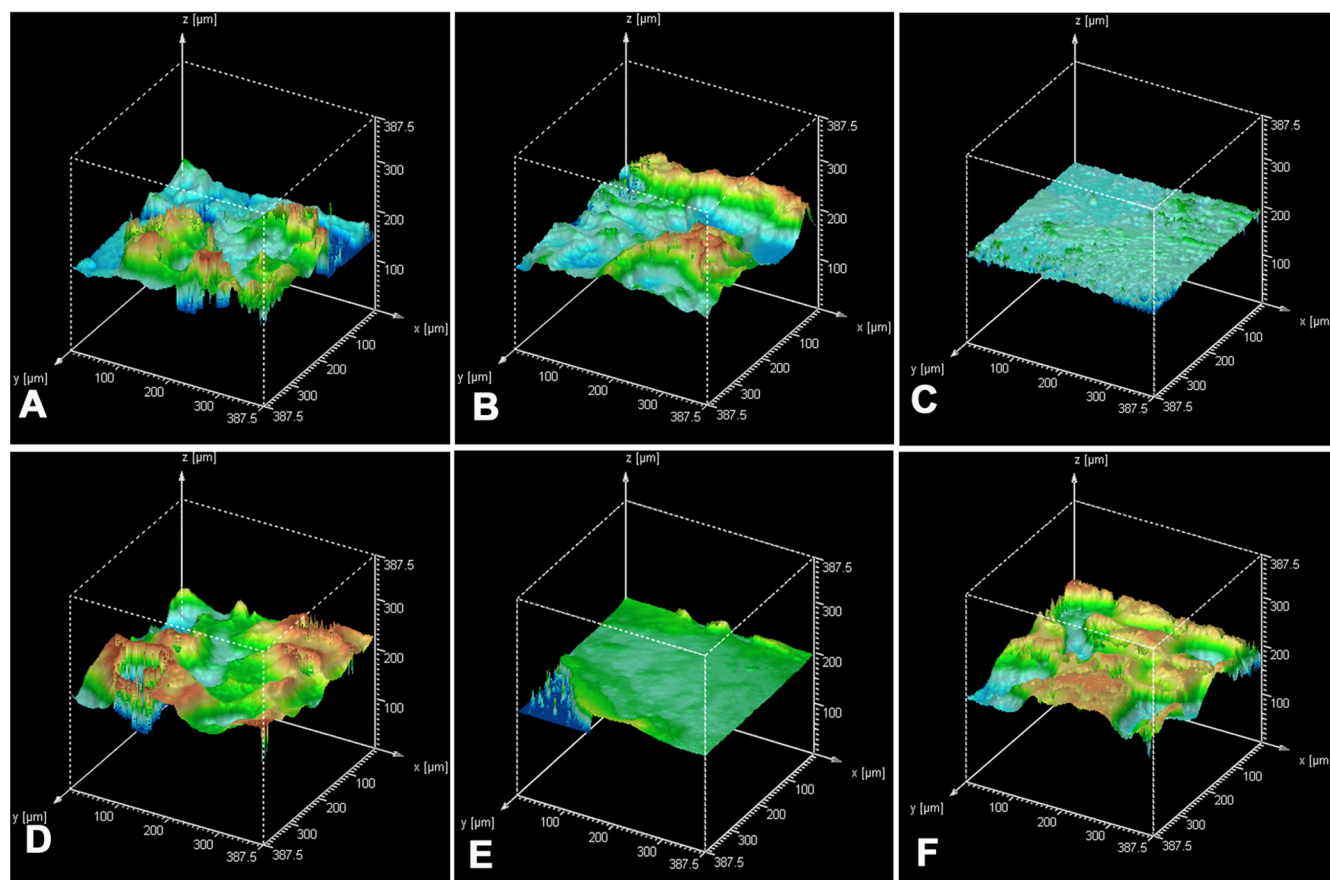


FIG. 3. Topographic reconstruction of colonies corresponding to those in Fig. 2. (A) *M. chubuense*. (B) *M. gilvum*. (C) *M. marinum*. (D) *M. obuense*. (E) *M. parafortuitum*. (F) *M. vaccae*. Evenness in color reflects uniformity of the colony surface. Strong variation in color shows high irregularity on the colony surface.

*t* test for comparison of means. Values of  $P > 0.05$  were considered statistically significant. All statistical procedures were performed using SPSS 15.0 software (SPSS Inc., Chicago, IL).

## RESULTS

**CLSM showed different types of colonial architectures among the rough colonies.** The original strains of *M. chubuense*, *M. gilvum*, *M. obuense*, *M. parafortuitum*, and *M. vaccae* used in this study formed smooth and rough colonies when cultured on TSA. Meanwhile, *M. marinum* formed only rough colonies (Fig. 1). When we observed the rough colonies with binocular stereomicroscopy, we noted that the *M. chubuense*, *M. gilvum*, *M. obuense*, and *M. vaccae* colonies had highly textured surfaces with marked wrinkles. On the other hand, *M. marinum* and *M. parafortuitum* formed flat colonies with less relief (Fig. 1). We decided to use CLSM to study these rough colonies in depth. Side views of the three-dimensional reconstructed images were used to determine the colony structure (Fig. 2). CLSM showed that the rough colonies of *M. chubuense*, *M. gilvum*, *M. obuense*, and *M. vaccae* had a more spatially heterogeneous structure, forming thick colonial cords (Fig. 2A, B, D, and F, respectively). This heterogeneity could also be discerned along the *z* axis on the *x-z* projection. However, the colonies of *M. marinum* and *M. parafortuitum* showed

a homogeneous flat structure (Fig. 2C and E). The presence of fine and flat colonial cords was clearly visualized in *M. marinum* (Fig. 2C), and no relief or cords were detected in the *M. parafortuitum* colonies (Fig. 2E). Smooth colonies of all the strains showed no contours or colonial cords (see Fig. S1 in the supplemental material).

Figure 3 shows the surface topography and uses a false-color scale to represent total depth, from blue (deepest valleys) to yellow (highest peaks). Irregularities in the surface are reflected by changes in color: strong variation in color indicates a very irregular surface, and evenness of color shows a uniform surface. All the rough colonies, with the exception of those of *M. marinum* and *M. parafortuitum* (Fig. 3C and E, respectively), showed prominent peaks and valleys with randomly distributed peaks.

**SEM showed that microscopic cords were present in all the spreading pellicles formed by the rough colonies.** Smooth and rough colonies of *M. chubuense*, *M. gilvum*, *M. obuense*, *M. parafortuitum*, and *M. vaccae*, as well as the rough colonies of *M. marinum* (Fig. 1), were cultured in TSB. *M. marinum* was included in the study as a positive-control strain for cording, since the observation of cords in this species (by optical microscopy) was previously described by others (11, 24). As shown in Fig. 1, the rough colonies inoculated into the TSB



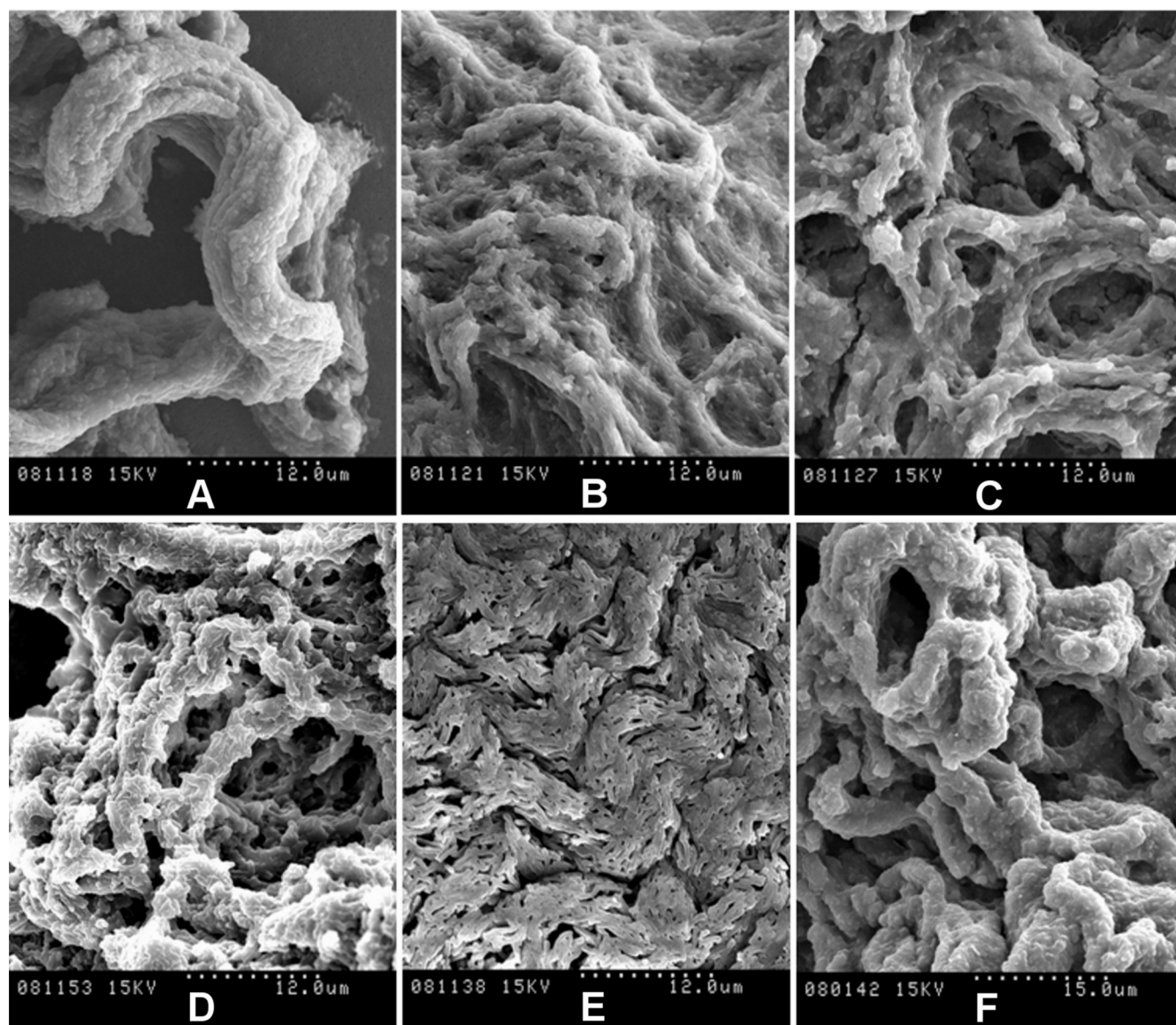


FIG. 4. Spreading pellicles fixed with osmium vapors show cords with native extracellular components. The SEM micrographs show the different cord morphologies formed in TSB liquid medium by rough colonies of *M. chubuense* (A), *M. gilvum* (B), *M. marinum* (C), *M. obuense* (D), *M. parafortuitum* (E), and *M. vaccae* (F). Note the large amounts of extracellular components covering the cells. These native components persisted in the samples due to being directly fixed with osmium vapors. The micrographs are representative of the general aspects of four different cultures.

grew as a spreading pellicle that climbed the walls of the glass tubes. On the other hand, the smooth colonies did not spread or climb but merely grew inside the medium, producing an appreciable precipitate at the bottom of the tube.

Cells for the Ziehl-Neelsen smear and SEM were taken from spreading pellicles (for the rough variants) or sediments (for the smooth variants). Figure 4 shows the SEM images obtained when the pellicles were fixed directly with osmium vapors. This process conserves the materials and structures very well and allows fragile structures to be observed at high magnification. We thus observed the presence of cords in all the spreading pellicles. *M. parafortuitum* (Fig. 4E) formed flat cords, while *M. chubuense* and *M. vaccae* formed large, prominent cords (Fig. 4A and F, respectively). Bacilli in the cords acted as cover for

an extracellular substance that was removed when the pellicles were fixed with glutaraldehyde and dehydrated with ethanol (Fig. 5 and 6). We were therefore able to clearly observe the bacilli packed end to end and side to side to form a cord in which the orientation of the long axis of each cell was parallel to the long axis of the cord.

The SEM images presented in this work are the first images in which it is possible to clearly observe this phenomenon (Fig. 5 and 6; see Fig. S3 in the supplemental material). Fine cords formed by a few bacilli were observed in *M. marinum* and *M. parafortuitum*, and according to the images obtained using direct fixation with osmium vapors, more robust cords formed by more bacilli were observed in the other species. No such clear and definitive images of the presence of cords were obtained

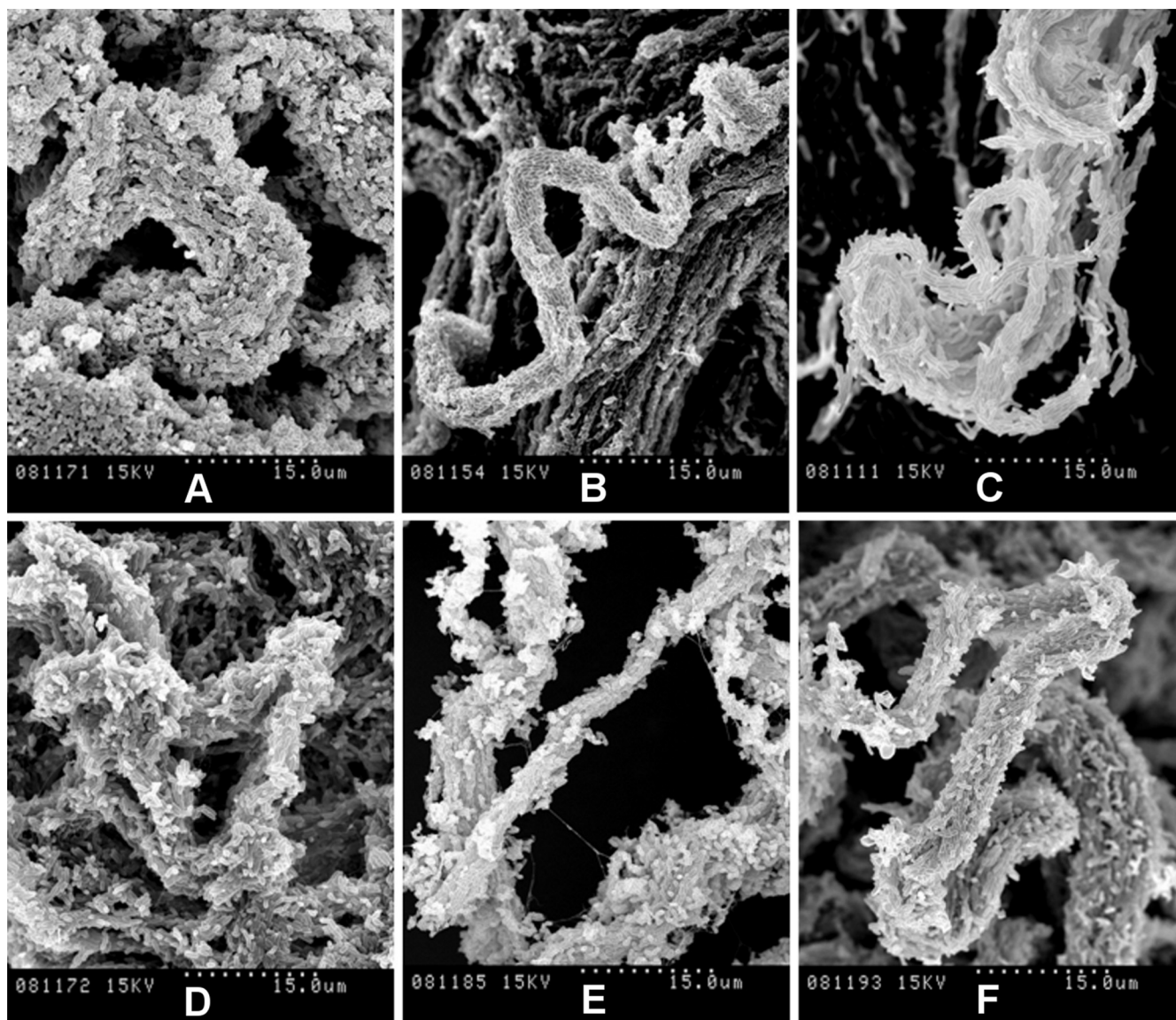


FIG. 5. Spreading pellicles fixed with conventional methods for SEM show the organization of bacilli in the cords. Shown are SEM micrographs of cords formed in liquid medium by rough colonies of *M. chubuense* (A), *M. gilvum* (B), *M. marinum* (C), *M. obuense* (D), *M. parafortuitum* (E), and *M. vaccae* (F). The samples were processed following conventional SEM procedures of fixation with aldehydes, and the extracellular components are greatly extracted, rendering the cell surface visible. Note the differences in cord morphology among the species. The images are representative of images obtained from four different cultures.

with optical microscopy (see Fig. S2 in the supplemental material).

SEM of sediments from smooth mycobacteria that grew inside the TSB medium revealed masses of bacterial cells without orientation, and empty spaces were clearly visible among the single cells (see Fig. S4 in the supplemental material). In Figure S4, we show only the images obtained of the smooth *M. vaccae*, since the images obtained of the smooth morphotypes of the other species studied were very similar.

**Increased survival of rough cording morphotypes in J774 macrophages compared to smooth noncording morphotypes.** J774, a murine monocyte/macrophage cell line, enables comparative studies of virulence among mycobacterial strains in a homogeneous population to be carried out. This cell line is widely used

in pathogenicity studies, and the behavior of pathogenic and nonpathogenic species in J774 cells is well known (7, 14, 20, 27). In order to investigate the relationship between cord formation and virulence, the J774 macrophage cell line was infected with *M. marinum* and each variant of the five different RGSM species, and their intracellular survival was tested by measuring intracellular CFU by plating macrophage lysates over a 96-hour period. A significant increase in the survival of bacilli from rough colonies was detected for all species ( $F = 255,049$ ;  $P < 0.001$ ).

As Fig. 7 shows, *M. marinum* survived inside macrophages, but it did not replicate, leading to a steady decline in the viable counts. This is the typical behavior described for this species in the J774 cell line when cultures were produced at 37°C (20).



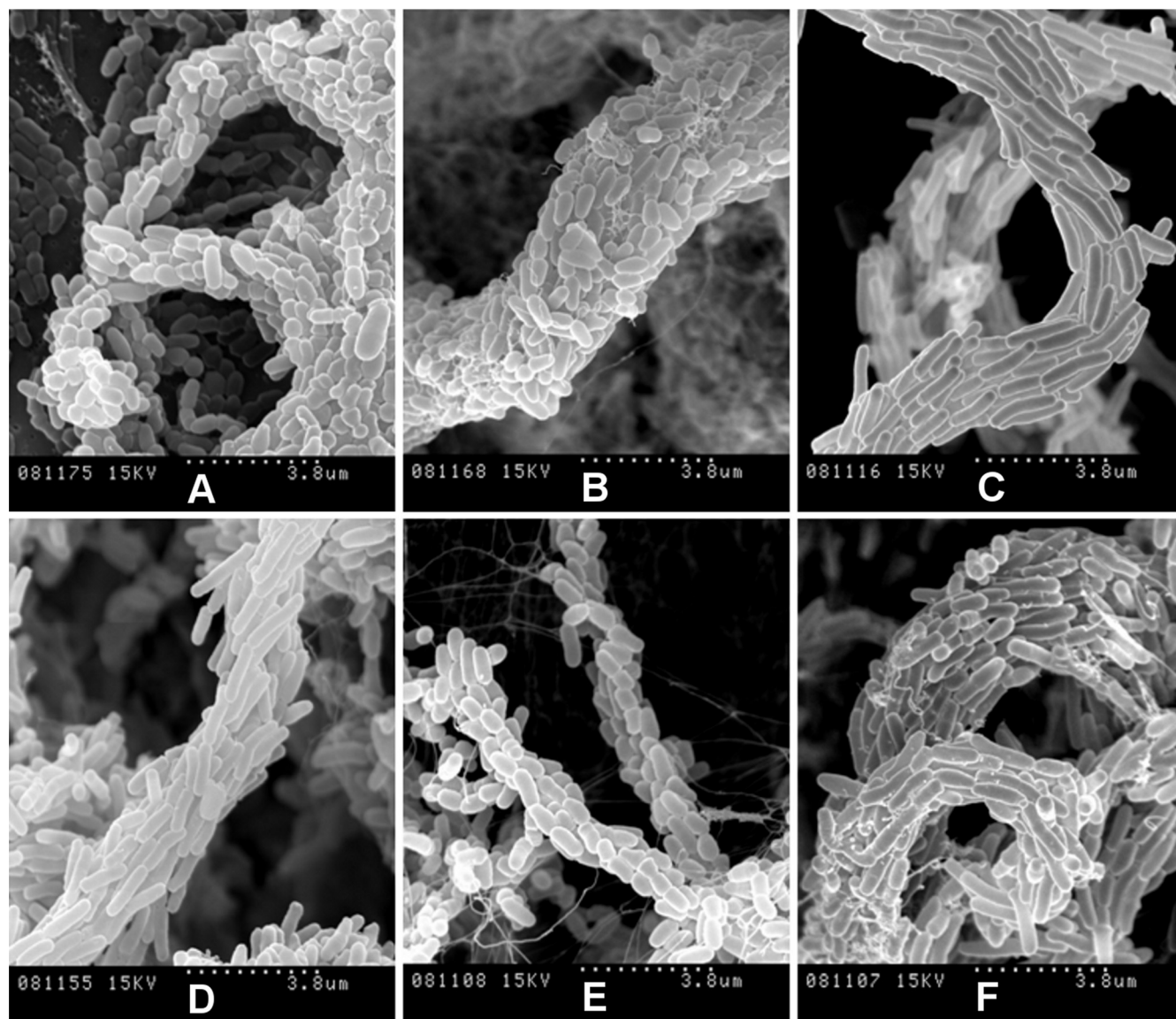


FIG. 6. High magnification of spreading pellicles, fixed with conventional methods for SEM, with bacilli arranged along the long axis of the cord. SEM micrographs at high magnification show details of cords formed in liquid medium by rough colonies of *M. chubuense* (A), *M. gilvum* (B), *M. marinum* (C), *M. obuense* (D), *M. parafortuitum* (E), and *M. vaccae* (F) in samples processed following conventional SEM procedures of fixation with aldehydes. The images are representative of images obtained from four different cultures.

The abilities of the other strains to persist inside macrophages varied depending on the species and the colonial morphology. Interestingly, the smooth variants of all the RGSM species showed impaired intracellular survival compared to the rough variants (Fig. 7). Eight hours after infection, the J774 cell line killed the smooth variants more rapidly than the rough variants. After 24 h, the differences in the abilities to persist inside macrophages increased by about 1 to 2 log units in the rough variants compared to the respective smooth variants. In all cases, the number of mycobacterial cells decreased over time, but at the end of the experiments (96 h), and with the sole exception of *M. parafortuitum*, survival was statistically significantly higher in the rough than in the smooth variants. In all cases, rough strains emerged from macrophage infection as rough again.

## DISCUSSION

We started this work with the aim of inquiring whether rough colonies of RGSM were able to produce microscopic cords, a characteristic that is considered a virulence factor in the genus *Mycobacterium*. In *M. tuberculosis* complex strains, microscopic cording observed in liquid medium by optical microscopy has been correlated with highly textured colonies that form many wrinkles or serpentine when grown on agar surfaces (9, 13, 16). This pattern of growth has also been described in *M. abscessus* (12). The combination of CLSM and SEM enabled us to affirm that rough wrinkled colonies of *M. chubuense*, *M. gilvum*, *M. obuense*, and *M. vaccae* formed microscopic cords when cultured in a liquid medium but rough colonies of *M. parafortuitum* and *M.*

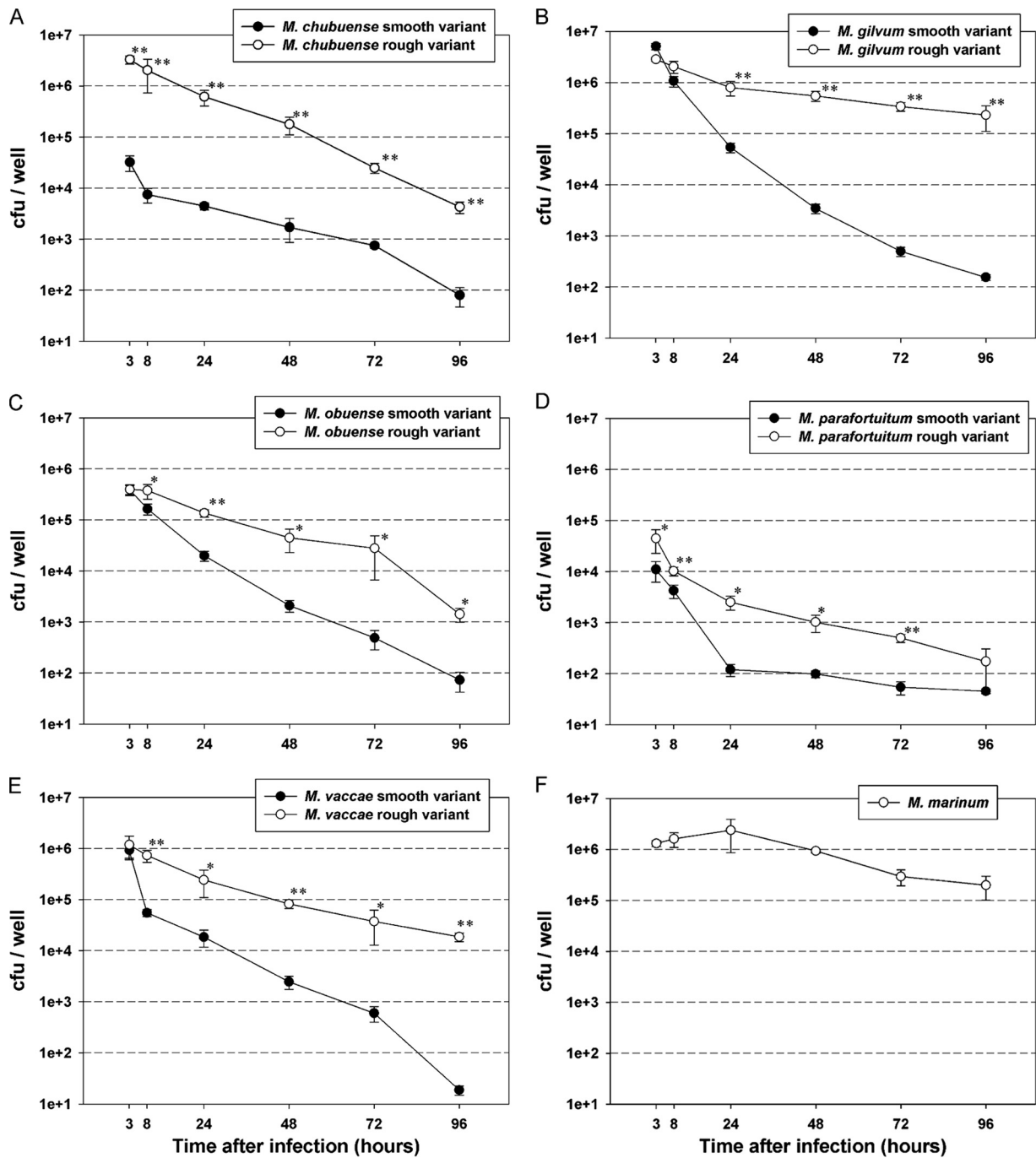


FIG. 7. Increased survival of rough cording morphotypes in J774 macrophages compared with smooth noncording morphotypes. J774 macrophages were infected with the smooth (●) or rough (○) variants of *M. chubuense* (A), *M. gilvum* (B), *M. obuense* (C), *M. parafortuitum* (D), and *M. vaccae* (E) and the *M. marinum* rough strain (F). At 3, 8, 24, 48, 72, and 96 h after infection, the supernatants were removed and serial dilutions of lysed macrophages were plated on TSA plates. Each time point represents the average colony counts  $\pm$  SD from three serial dilutions from each triplicate well of infected macrophage cultures. The data are representative of one out of three independent experiments. \*,  $P < 0.05$ ; \*\*,  $P < 0.001$  (unpaired Student's  $t$  test).

*marinum* that displayed flat morphologies without appreciable relief also formed microscopic cords when cultured in a liquid medium (Fig. 1 to 6). The initial conclusion of this work, therefore, is that the architecture of rough colonies is not correlated with microscopic cording, since both flat and

wrinkled colonies formed microscopic cords in liquid medium.

Microscopic cording, in RGSM and *M. marinum*, was observed by means of the SEM and the Ziehl-Neelsen stain performed on the spreading pellicles that the rough colonies



formed when cultured in liquid medium. The discovery that virulent tubercle bacilli grew on the surface of a liquid medium, forming veils that spread uniformly over the entire surface of the liquid medium, and climbed up the sides of the glass container, was first described by Koch in 1884 and later by others as a typical characteristic of *M. tuberculosis* complex strains. Cording in these pellicles was observed by optical microscopy and traditional stains (9, 13, 15, 16, 19). The formation of spreading pellicles has been extensively studied in the nonpathogenic species *M. smegmatis*, in which it has been related to iron availability, synthesis of short-chain mycolic acids, and synthesis of mycolyl-diacylglycerols (4, 18). However, no studies relating the formation of spreading pellicles to the formation of microscopic cords have been performed in *M. smegmatis*. The formation of spreading pellicles has not been reported in *M. marinum* and *M. abscessus*, the other two species in which microscopic cording has been reported (12, 24). Our second conclusion is that rough RGSM and *M. marinum* also form spreading pellicles and that the formation of these is linked to the formation of microscopic cords (Fig. 1 and Fig. 4 to 6; see Fig. S3 in the supplemental material).

Smooth colonies of RGSM were unable to grow on the surface of the liquid medium, and SEM of sediments revealed that they were also unable to form cords (Fig. 1; see Fig. S4 in the supplemental material). The application of SEM to the study of the pellicles clearly showed that they all contained cords and that the volume, thickness, prominence, and architecture of cords were different among the species (Fig. 4 to 6; see Fig. S3 in the supplemental material). Cording has previously been studied only with optical microscopy, using mainly Ziehl-Neelsen, Kinyoun, and auramine rhodamine stains (9, 13, 24). In this work, SEM was applied to the study of cords for the first time, providing the first images that enable the ultrastructure of these characteristic formations to be observed. Whether a strain produces cords can be categorically determined by SEM, significantly improving on the observations performed with optical microscopy (see Fig. S2 in the supplemental material) and showing cord images of high definition and quality. Our results demonstrate that SEM is a powerful tool for detecting the presence and morphology of cords in mycobacteria. Our third conclusion is that SEM is the best technique for studying microscopic cording.

Natural or constructed mutants of the *M. tuberculosis* complex species, *M. marinum*, and *M. abscessus* that were unable to form microscopic cords showed impaired virulence compared to the original cording strains (6, 8, 9, 12, 16). Virulence in mycobacteria is associated with the ability of the bacterial cells to survive in host macrophages (7, 14, 20, 22, 23, 27, 29). The J774 mouse macrophage cell line is one of the most frequently used tools for comparative studies of virulence among mycobacterial strains (7, 14, 20, 27). When we compared survival in J774 macrophages between rough cording and noncording smooth colonies of RGSM, we found that mycobacteria from rough colonies persisted longer than those from smooth colonies inside macrophages. These results support the role of microscopic cording in the virulence of mycobacteria.

In summary, we have studied rough colony mutants of *M. chubuense*, *M. gilvum*, *M. obuense*, *M. parafortuitum*, and *M. vaccae* strains, demonstrating that, unlike the smooth mutants,

all the rough mutants formed spreading pellicles that contained microscopic cords.

To date, microscopic cords have been described only in the *M. tuberculosis* complex, *M. marinum*, and rough *M. abscessus*. We have described this phenomenon for the first time in other mycobacterial species belonging to the RGSM group. Although microscopic cording had been related to rough wrinkled colonies in the *M. tuberculosis* complex and in *M. abscessus*, we used CLSM and SEM to show that flat colonies without wrinkles or other contours also produce microscopic cords when cultured in a liquid medium. The SEM techniques used in this work allowed us to ascertain whether mycobacteria produce cords, to obtain detailed images of their ultrastructure, and to establish that cording ultrastructure differences among the species studied exist. Finally, we showed that rough cording colonies persisted longer in cultured macrophages than the original smooth noncording ones.

We believe that the results presented in this work open up many new possibilities for the study of cords, a virulence factor of historical significance in mycobacteriology that intrigues *Mycobacterium* cell envelope researchers. Furthermore, this study improves our understanding of the biology of different species of the genus *Mycobacterium*, which could contribute to a better understanding of how *M. tuberculosis* and other mycobacteria cause disease.

#### ACKNOWLEDGMENTS

This work was supported by the Spanish MCT (SAF2002-005149), MEC (SAF2006-05868), and Catalan AGAUR (2005SGR00956).

We thank Carlos Martín for providing the J774 cell line. We also thank Rita López and Francesc Bohils (Microscopy Service, UAB) for their laboratory assistance.

#### REFERENCES

- Agustí, G., O. Astola, E. Rodríguez-Güell, E. Julián, and M. Luquin. 2008. Surface spreading motility by a group of phylogenetically related rapidly growing pigmented mycobacteria suggests that motility is a common property of mycobacterial species but is restricted to smooth colonies. *J. Bacteriol.* **190**:6894–6902.
- Bloch, H., E. Sorkin, and H. Erlenmeyer. 1953. A toxic lipid component of the tubercle bacillus (cord factor). I. Isolation from petroleum ether extracts of young bacterial cultures. *Am. Rev. Tuberc.* **67**:629–643.
- Catherinot, E., A. L. Roux, E. Macheras, D. Hubert, M. Matmar, L. Dannhoffer, T. Chinnet, P. Morand, C. Poyart, B. Heym, M. Rottman, J. L. Gailhard, and J. L. Herrmann. 2009. Acute respiratory failure involving an R variant of *Mycobacterium abscessus*. *J. Clin. Microbiol.* **47**:271–274.
- Chen, J. M., G. J. German, D. C. Alexander, H. Ren, T. Tan, and J. Liu. 2006. Roles of Lsr2 in colony morphology and biofilm formation of *Mycobacterium smegmatis*. *J. Bacteriol.* **188**:633–641.
- Dhariwal, K. R., Y. M. Yang, H. M. Fales, and M. B. Goren. 1987. Detection of trehalose monomycolate in *Mycobacterium leprae* grown in armadillo tissues. *J. Gen. Microbiol.* **133**:201–209.
- Ferrer, N. L., A. B. Gómez, C. Y. Soto, O. Neyrolles, B. Gicquel, F. García-Del Portillo, and C. Martín. 2009. Intracellular replication of attenuated *Mycobacterium tuberculosis phoP* mutant in the absence of host cell cytotoxicity. *Microbes Infect.* **11**:115–122.
- Gao, L. Y., F. Laval, E. H. Lawson, R. K. Groger, A. Woodruff, J. H. Morisaki, J. S. Cox, M. Daffé, and E. J. Brown. 2003. Requirement for *kasB* in *Mycobacterium* mycolic acid biosynthesis, cell wall impermeability and intracellular survival: implications for therapy. *Mol. Microbiol.* **49**:1547–1563.
- Glickman, M. S. 2008. Cording, cord factors, and trehalose dimycolate, p. 63–73. In M. Daffé and J. M. Reyrat (ed.), *The mycobacterial cell envelope*. ASM Press, Washington, DC.
- Glickman, M. S., J. S. Cox, and W. R. Jacobs. 2000. A novel acid cyclopropane synthetase is required for cording, persistence, and virulence of *Mycobacterium tuberculosis*. *Mol. Cell* **5**:717–727.
- Hachem, R., I. Raad, K. V. Rolston, E. Whimbey, and R. Katz. 1996. Cutaneous and pulmonary infections caused by *Mycobacterium vaccae*. *Clin. Infect. Dis.* **23**:173–175.

11. Hall-Stoodley, L., O. S. Brun, G. Polshyna, and L. P. Barker. 2006. *Mycobacterium marinum* biofilm formation reveals cording morphology. *FEMS Microbiol. Lett.* **257**:43–49.
12. Howard, S. T., E. Rhoades, J. Recht, X. Pang, A. Alsop, R. Kolter, C. R. Lyons, and T. F. Byrd. 2006. Spontaneous reversion of *Mycobacterium abscessus* from a smooth to a rough morphotype is associated with reduced expression of glycopeptidolipid and reacquisition of an invasive phenotype. *Microbiology* **152**:1581–1590.
13. Hunter, R. L., N. Venkataprasad, and M. R. Olsen. 2006. The role of trehalose dimycolate (cord factor) on morphology of virulent *Mycobacterium tuberculosis* in vitro. *Tuberculosis* **86**:349–356.
14. Indrigo, J., R. L. Hunter, and J. K. Actor. 2003. Cord factor trehalose 6,6'-dimycolate (TDM) mediates trafficking events during mycobacterial infection of murine macrophages. *Microbiology* **149**:2049–2059.
15. McCarter, Y. S., I. N. Ratkiewicz, and A. Robinson. 1998. Cord formation in BACTEC medium is a reliable, rapid method for presumptive identification of *Mycobacterium tuberculosis* complex. *J. Clin. Microbiol.* **36**:2769–2771.
16. Middlebrook, G., R. J. Dobos, and C. Pierce. 1947. Virulence and morphological characteristics of mammalian tubercle bacilli. *J. Exp. Med.* **86**:175–184.
17. Noll, H., and H. Bloch. 1955. Studies on the chemistry of the cord factor of *Mycobacterium tuberculosis*. *J. Biol. Chem.* **214**:251–265.
18. Ojha, A., and G. F. Hatfull. 2007. The role of iron in *Mycobacterium smegmatis* biofilm formation: the exochelin siderophore is essential in limiting iron conditions for biofilm formation but not for planktonic growth. *Mol. Microbiol.* **66**:468–483.
19. Ojha, A. K., A. D. Baughn, D. Sambandan, T. Hsu, X. Trivelli, Y. Guerardel, A. Alahari, L. Kremer, W. R. Jacobs, Jr., and G. F. Hatfull. 2008. Growth of *Mycobacterium tuberculosis* biofilms containing free mycolic acids and harbouring drug-tolerant bacteria. *Mol. Microbiol.* **69**:164–174.
20. Ramakrishnan, L., and S. Falkow. 1994. *Mycobacterium marinum* persists in cultured mammalian cells in a temperature-restricted fashion. *Infect. Immun.* **62**:3222–3229.
21. Rodríguez-Güell, E., G. Agustí, M. Corominas, P. J. Cardona, I. Casals, T. Parella, M. A. Sempere, M. Luquin, and E. Julián. 2006. The production of a new extracellular putative long-chain saturated polyester by smooth variants of *Mycobacterium vaccae* interferes with Th1-cytokine production. *Antonie Van Leeuwenhoek* **90**:93–108.
22. Rohde, K., R. M. Yates, G. E. Purdy, and D. G. Russell. 2007. *Mycobacterium tuberculosis* and the environment within the phagosome. *Immunol. Rev.* **219**:37–54.
23. Smith, I. 2003. *Mycobacterium tuberculosis* pathogenesis and molecular determinants of virulence. *Clin. Microbiol. Rev.* **16**:463–496.
24. Staropoli, J. F., and J. A. Branda. 2008. Cord formation in a clinical isolate of *Mycobacterium marinum*. *J. Clin. Microbiol.* **46**:2814–2816.
25. Stinear, T. P., T. Seemann, P. F. Harrison, G. A. Jenkin, J. K. Davies, P. D. Johnson, Z. Abdellah, C. Arrowsmith, T. Chillingworth, C. Churcher, K. Clarke, A. Cronin, P. Davis, I. Goodhead, N. Holroyd, K. Jagels, A. Lord, S. Moule, K. Mungall, H. Norbertczak, M. A. Quail, E. Rabinowitsch, D. Walker, B. White, S. Whitehead, P. L. Small, R. Brosch, L. Ramakrishnan, M. A. Fischbach, J. Parkhill, and S. T. Cole. 2008. Insights from the complete genome sequence of *Mycobacterium marinum* on the evolution of *Mycobacterium tuberculosis*. *Genome Res.* **18**:729–741.
26. Stokes, R. W., R. Norris-Jones, D. E. Brooks, T. J. Beveridge, D. Doxsee, and L. M. Thorson. 2004. The glycan-rich outer layer of the cell wall of *Mycobacterium tuberculosis* acts as an antiphagocytic capsule limiting the association of the bacterium with macrophages. *Infect. Immun.* **72**:5676–5686.
27. Tan, T., W. L. Lee, D. C. Alexander, S. Grinstein, and J. Liu. 2006. The ESAT-6/CFP-10 secretion system of *Mycobacterium marinum* modulates phagosome maturation. *Cell. Microbiol.* **8**:1417–1429.
28. Tortoli, E. 2006. The new mycobacteria: an update. *FEMS Immunol. Med. Microbiol.* **48**:159–178.
29. Young, D. B., M. D. Perkins, K. Duncan, and C. E. Barry III. 2008. Confronting the scientific obstacles to global control of tuberculosis. *J. Clin. Investig.* **118**:1255–1265.